

## Phenomenological local field enhancement factor distributions around electromagnetic hot spots

E. C. Le Ru<sup>a)</sup> and P. G. Etchegoin<sup>b)</sup>

*The MacDiarmid Institute for Advanced Materials and Nanotechnology, School of Chemical and Physical Sciences, Victoria University of Wellington, P.O. Box 600, Wellington 6140, New Zealand*

(Received 14 January 2009; accepted 28 April 2009; published online 14 May 2009)

We propose a general phenomenological description of the enhancement factor distribution for surface-enhanced Raman scattering (SERS) and other related phenomena exploiting large local field enhancements at hot spots. This description extends naturally the particular case of a single (fixed) hot spot, and it is expected to be “universal” for many classes of common SERS substrates containing a collection of electromagnetic hot spots with varying geometrical parameters. We further justify it from calculations with generalized Mie theory. The description studied here provides a useful starting point for a qualitative (and semiquantitative) understanding of experimental data and, in particular, the analysis of the statistics of single-molecule SERS events. © 2009 American Institute of Physics. [DOI: 10.1063/1.3138784]

There has been considerable progress lately on the interpretation of single-molecule surface-enhanced Raman scattering (SM-SERS) experiments.<sup>1–7</sup> Two salient aspects of the problem are: (i) the magnitude of the SERS enhancement factor (EF) needed to observe SM-SERS, which can be up to a million times smaller than what was previously deemed necessary ( $\sim 10^8$  instead of  $\sim 10^{14}$ );<sup>5–7</sup> and (ii) the existence of “extreme statistics” brought about by the long-tail nature of the distribution of SERS EFs around hot spots. This second issue has been studied in Ref. 1, wherein the EF distribution for a single (fixed) geometry defined by a dimer has been extensively explored. The latter was shown to be well-described by a truncated Pareto distribution—a special case of long-tail distributions. Real systems with multiple hot spots contributing to the signal (over space or time) are expected to be an “averaged version”—over the relevant geometrical parameters—of the single hot spot distribution. We focus here on the influence of this averaging process on the overall EF distribution deduced from a single hot spot. This averaged distribution is what is actually measured in most experiments.

As a point in case, there have been two recent attempts<sup>8,9</sup> at measuring this overall SERS EF distribution experimentally, a difficult undertaking in general. The long-tail nature of the distribution was indeed confirmed in both cases. Nevertheless, because of the intrinsic hot spot-to-hot spot variability, the actual probability distribution was (naturally) different from the simplest truncated Pareto distribution predicted for a single hot spot.<sup>1</sup> In Ref. 9, a modified probability distribution was in fact proposed to describe the data empirically. In this communication, we extend this phenomenological description and show how it can be connected to actual electromagnetic (EM) calculations (with Mie theory), by “averaging” the single hot spot EF distributions over the

relevant geometrical parameters of the problem. Ultimately, the objective of the paper is to provide (and justify) a heuristic representation of the SERS EF probability distribution in terms of a small number of parameters, which can be used subsequently to understand or predict aspects of many plasmonics and SERS experiments.

Let us start with a few defining aspects of EM local field EFs at hot spots. We use the canonical example of a dimer as shown in Fig. 1(a) to highlight the basic ideas and set the ground for the forthcoming discussion. Two metallic particles of same radius  $a$  separated by a short distance  $d$  form an EM hot spot in the gap, i.e., a highly localized region where the local field enhancements (and therefore the SERS EF) may be very large under appropriate excitation conditions (wavelength and polarization). The SERS EF ( $F$ ) is typically largest along the axis joining the two particles, while its probability distribution exhibits a long tail with a cutoff corresponding to the maximum SERS EF exactly at the hot spot. This can for example be described by three parameters when approximated by a truncated Pareto distribution.<sup>1</sup> This distribution is shown schematically in Fig. 1(b) (black line) in terms of  $p(L=\log_{10}(F))$ . It reflects the possible values of  $L$  (or  $F$ ) for molecules randomly distributed on the surface of the particles.<sup>1</sup>

Except for special situations (like tip-enhanced Raman scattering<sup>10</sup>) where the properties of a single hot spot are measured, the most common situation is to sample SERS signal from a substrate displaying variations from hot spot to hot spot belonging to a certain family. As a way of example, we can mention the random hot spots that are produced in colloidal clusters in liquids<sup>11</sup> or on dry substrates generated by grafting clusters onto planar substrates.<sup>7,12</sup> Both cases represent a situation where hot spots belong to a certain “family” sharing common general characteristics (typical sizes of particles, typical gaps among particles, etc.). However, naturally, not all hot spots will be the same, and there will be a distribution of parameters, i.e., size, gap, shape, orientation,

<sup>a)</sup>Electronic mail: eric.leru@vuw.ac.nz.

<sup>b)</sup>Electronic mail: pablo.etchegoin@vuw.ac.nz.

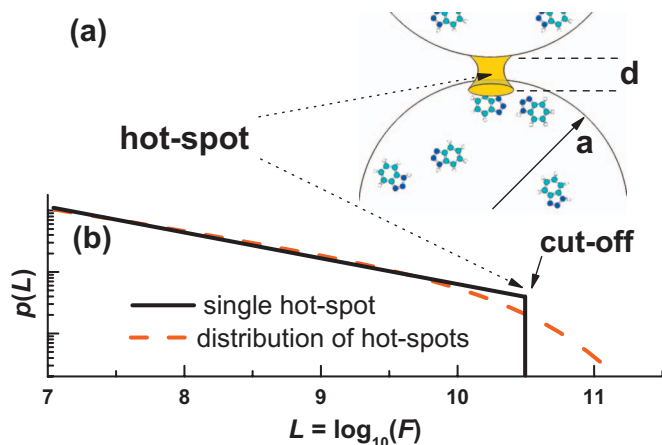


FIG. 1. (Color) (a) Schematic plot of the main geometrical aspects of an EM hot spot formed by a dimer. The surface of the particles are schematically shown with a small number of molecules (not to scale) at random positions, thus exploring different values of the EF distribution in the dimer. (b) Long-tail distribution of SERS EFs ( $F$ ) with a cutoff for a fixed geometry,  $a = 30$  nm,  $d = 1.3$  nm (single hot spot—black solid line), and for a collection of different hot spots (multiple hot spot—dashed red line). The dashed curve represents the EF distribution that the molecules will experience when adsorbed at a random position on a dimer where the geometrical parameters [ $a$  and  $d$  in Fig. 1(a)] are randomly chosen within a certain range. We will show how we can go from the single (black curve) to the multiple hot spot distribution (red dashed curve) by a suitable averaging over dimers with different gaps  $d$  and radii  $a$  [Fig. 1(a)].

etc. The most obvious effect of such variability will be the resulting variation in the *maximum* SERS EF,  $F_{\max}$  from hot spot to hot spot (because of different resonance condition, gaps, or orientation). This is explicitly demonstrated on an example in Fig. 2 (discussed later on). Such changes in  $F_{\max}$  will qualitatively “blur” the cutoff in the EF distribution, and this is associated with a change in the slope of the distribution for large SERS EF as shown schematically in Fig. 1(b) (dashed red curve). This effect has, in fact, been measured experimentally<sup>8,9</sup> for two different types of SERS substrate. Furthermore, in Ref. 9, an empirical SERS EF distribution was proposed,

$$p(F) = AF^{-(1+k)} \exp[-(F/F_0)^\eta], \quad (1)$$

with  $k=0.75$  and  $\eta=0.25$ . These particular values were deduced from the empirical observation that the probability distribution of  $F^{1/4}$  was approximately exponential. We propose here to keep  $k$  and  $\eta$  as free parameters along with  $A$  and  $F_0$ , the latter now playing a role similar to that of  $F_{\max}$  for the truncated Pareto distribution. Equation (1) then describes phenomenologically the EF distribution of a broad class of plasmonic substrates with blurred cutoff. It is a generalization of the truncated Pareto distribution proposed in Ref. 1, toward which it formally converges for large  $\eta$ . In fact, the cutoff is more marked for larger  $\eta$  and becomes less and less important as  $\eta$  tends to zero (for which a nontruncated Pareto distribution is obtained). This distribution has a crossover from a *power law*, like the truncated Pareto distribution of a single hot spot, to a *stretched exponential* behavior for the largest  $F$ 's. As for the truncated Pareto distribution, a minimum SERS EF,  $F_{\min}$ , must be artificially introduced for mathematical consistency,<sup>1</sup> i.e., to normalize the probability distribution  $p(F)$ , but it has no physical im-

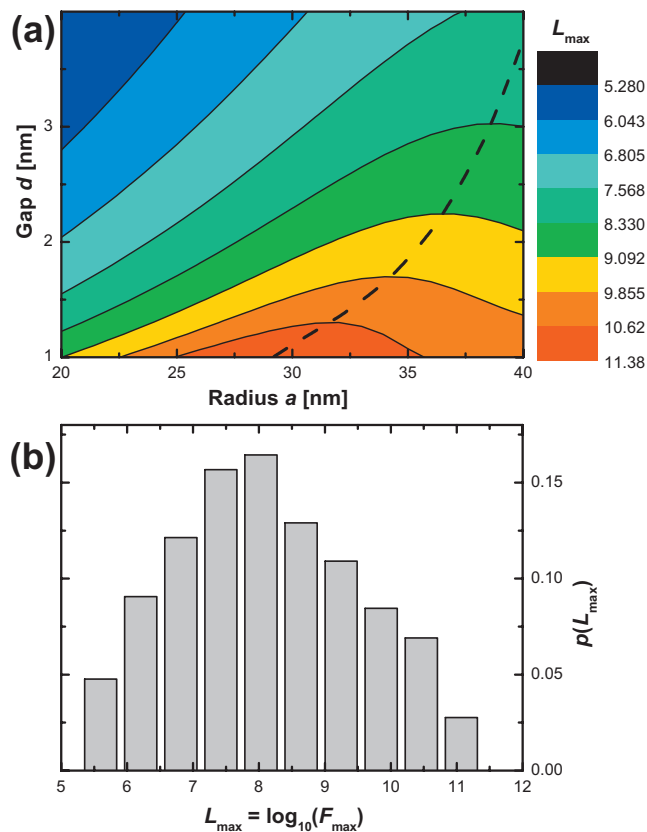


FIG. 2. (Color) (a) Maximum SERS EF,  $F_{\max}$ , on the surface in the gap of a dimer, as a function of the geometrical parameters, radius, and gap.  $L_{\max} = \log_{10}(F_{\max})$  is used here for visualization purposes. (b) Corresponding probability distribution of  $L_{\max}$  (note that this is specific to the range of parameters considered here).

plications, all physical properties are determined by the tail of the distribution (large EFs). For example, the average SERS EF is

$$\langle F \rangle \approx \frac{A}{\eta} F_0^{1-k} \Gamma\left(\frac{1-k}{\eta}\right), \quad (2)$$

where  $\Gamma$  is the gamma function. As expected, this expression reduces to Eq. (A6) of Ref. 1 as  $\eta \rightarrow +\infty$ .

We believe that a distribution of the type given in Eq. (1) can accommodate a large number of cases found in practice by combining the two essential elements: (i) the long-tail nature ( $\sim F^{-(1+k)}$ ) arising already for a single hot spot and (ii) a “blurring” of the cutoff of the distribution (modeled in this case by a stretched exponential  $\sim \exp[-(F/F_0)^\eta]$ ) arising from the hot spot-to-hot spot variations. These two key elements will be present in a vast number of systems, albeit with (possibly) different exponents ( $k, \eta$ ), which will have to be characterized on a case-by-case basis.

We now show a specific example of how a phenomenological distribution such as Eq. (1) can be derived from the EM theory of SERS EFs,<sup>1,7</sup> by a suitable averaging over the relevant geometrical parameters of a collection of hot spots. The example is a simplified version of what happens in a partially aggregated colloidal SERS substrate. The geometrical characteristics of citrate-reduced Lee and Meisel<sup>13</sup> Ag colloids are well known. Ignoring some shape dispersion, most particles can be seen as “spheres” of an average radius

$\sim 30$  nm.<sup>11</sup> For the sake of argument, we consider a distribution of dimers with radii between  $20 \text{ nm} < a < 40 \text{ nm}$  and gaps between  $1 \text{ nm} < d < 4 \text{ nm}$  (1 nm is a typical minimum size for dyes and gaps larger than  $\sim 4$  nm render EFs that are too small to be relevant). In order to give the calculation some resemblance to actual experimental situations, the dimers are immersed in water (index of refraction  $n=1.33$ ) and the laser excitation wavelength is chosen as 633 nm. A schematic representation with the main geometrical characteristics was shown in Fig. 1(a). The EM problems are solved using generalized Mie theory<sup>14,15</sup> (GMT) using the same parametrization of the dielectric function of Ag as in Ref. 1 (we assume a local dielectric response with no finite size corrections for electron scattering at the particle surface). GMT is particularly suited for this problem and renders results that can be considered as *exact* (within the approximation of the truncation of the series<sup>1</sup>). Moreover, EFs are calculated on the particle surface within the  $|E|^4$ -approximation<sup>16</sup> for zero Raman shift, which gives a good yardstick estimation of  $F$  regardless of some limitations that are well understood.<sup>7,16–18</sup> We first consider only one incident direction for the incoming wave:  $\perp$  to  $z$  (the main axis of the dimer) with a polarization  $\parallel$  to  $z$ . This configuration maximizes the enhancement at the hot spot.<sup>1,15</sup>

We first focus on the maximum SERS EF,  $F_{\max}$ , for each configuration, i.e., the SERS EF on the surface in the gap (along the dimer axis).  $F_{\max}$  obviously varies with the geometrical parameters, as shown in Fig. 2(a). This dependence reflects the two dominant EM contributions to the SERS EF. (i) First, the resonance condition: the resonance wavelength redshifts as either the gap decreases or the size increases.<sup>7</sup> At a fixed wavelength of 633 nm and for a gap of 1 nm, a radius of  $\approx 30$  nm offers the best resonance condition. As the gap increases, larger spheres are then necessary to remain at resonance. This effect is evident in Fig. 2(a) and further highlighted by the dashed line following the resonance condition. (ii) Second, smaller gaps result in larger field enhancements and this is also clear in the figure; highest SERS EFs are obtained for the smallest gaps, even when the resonance condition is not exactly met. In addition, the distribution of  $F_{\max}$  is shown in Fig. 2(b) as a complementary representation of the same results. Both plots re-emphasize the fact that large variations in  $F_{\max}$  are expected when considering a collection of hot spots, even for minute changes in the geometrical parameters.

Let us now focus on the full SERS EF distribution for the same collection of hot spots, i.e., we now consider the SERS EF at any random position on the surface, not only in the gap where it is largest. As discussed in Ref. 1, there are (at least) two approaches to obtain the SERS EF distribution for a given single hot spot. The first is to calculate the SERS EF distribution on the surface (for example as a function of  $\theta$  and  $\phi$ ), from which the probability distribution  $p(F)$  may be deduced, assuming a uniform distribution of molecules on the surface. The second is a Monte Carlo-type approach. Many positions are chosen randomly on the surface, and the SERS EF is calculated there. The histogram of the resulting  $F$ s (or  $L$ s) then represents  $p(F)$  [or  $p(L)$ ]. By its very nature, a long-tail distribution is very difficult to sample, and the

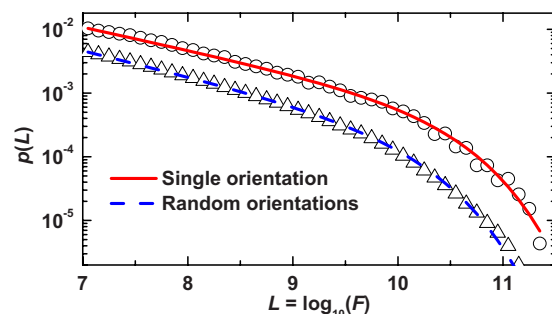


FIG. 3. (Color online) Calculations (symbols) and fits (lines) of the EF distribution for a collection of silver dimers chosen randomly from  $20 \text{ nm} < a < 40 \text{ nm}$  and  $1 \text{ nm} < d < 4 \text{ nm}$  (see Fig. 1). First, the incident wave vector is kept  $\perp$  to main axes of the dimer  $z$  and the polarization  $\parallel$  to  $z$  (circles). Then, random orientations of the dimers are considered (triangles). These EF distributions exhibit blurring of the cutoff in  $p(L)$  with a change in slope at high EFs.

Monte Carlo approach therefore requires to accumulate a large sample, typically more than  $10^5$  events. Nevertheless, this latter approach is more suited to the case considered here of many different hot spots. We can first fix the hot spot geometrical parameters and calculate  $F$  at a smaller number of random positions; ranging here from  $15 \times 10^3$  for  $a = 20 \text{ nm}$  to  $6 \times 10^4$  for  $a = 40 \text{ nm}$  (since it must scale with the surface area of the dimer). We then repeat the process for many (651 here) different hot spot parameters (radius and gap here). In this way, we obtain enough events ( $\sim 2.3 \times 10^7$  in our case) to guarantee a sound statistics of the poly-disperse system without having to calculate accurately the EF distribution for each individual hot spot. The resulting predicted distribution is shown in Fig. 3 as circles, along with a fit using Eq. (1) (solid line). The fit parameters are  $\eta=0.36$ ,  $k=0.64$ ,  $A=1.56$ , and  $F_0=2.8 \times 10^{10}$ . Note that we have set  $\eta+k=1$  for simplicity, but this may not be possible for other EF distributions. It is worth noting also that reasonably good fits may be obtained with different sets of parameters. For example, choosing first  $\eta=0.25$ , we find that  $A=0.096$ ,  $k=0.16$ , and  $F_0=2.5 \times 10^8$  results in a similar fit except for the last two points (largest EF). For our purpose here, the choice of parameters is not critical as long as it fits the distribution in the range of interest (i.e., the large EF tail). In fact, both sets predict using Eq. (2) the same average SERS EF of  $\langle F \rangle \approx 1.2 \times 10^7$ .

Finally, in many real situations where a collection of hot spots is sampled, the orientation of the hot spot axes will be random, and not aligned along the incident polarization (as considered so far). Other incident polarizations and directions produce in a first approximation a “scaled-down” version of what happens for this one. This is linked to the mainly *uniaxial* character of the coupled plasmon resonance producing the largest enhancements at the hot spot.<sup>1,18</sup> Following the same approach as in Ref. 1, we can predict the SERS EF distribution for the same collection of hot spots as before, but with random axis orientation. This is also shown in Fig. 3 (triangles), again with a fit (dashed line) using Eq. (1). The fit parameters are now  $\eta=0.6$ ,  $k=0.4$ ,  $A=1.28$ , and  $F_0=1.3 \times 10^{10}$ . The orientation averaging results, as intuitively expected, in a scaling of the SERS EF magnitudes;

the average SERS EF is reduced to  $\langle F \rangle \approx 2.5 \times 10^6$ . There is also a very slight “rounding off” of the cutoff region. Both effects are well-modeled by the phenomenological description of Eq. (1).

In closing, we have established a connection between a phenomenological description of the distribution of SERS EFs in systems with varying hot spots [Eq. (1)] and a microscopic derivation based on GMT predictions. As can be appreciated in Fig. 3, the predicted EF distributions can be modeled really well by Eq. (1), and other systems like the one studied experimentally in Ref. 9 follow the same law, albeit with different parameters. We believe this phenomenological description is therefore well suited to accommodate a wide range of plasmonic and SERS substrates composed of a collection of hot spots, and it is both justified by experimental findings<sup>9</sup> and a generalization of the earlier work on single hot spots.<sup>1</sup> Ultimately, Eq. (1) can be taken as a heuristic approach to describe real systems and can be used to quantify/compare different situations/substrates or produce predictions on the statistics of SM-SERS events.

We are indebted to the Royal Society of New Zealand for partial financial support under a Marsden Grant.

- <sup>1</sup>E. C. Le Ru, P. G. Etchegoin, and M. Meyer, *J. Chem. Phys.* **125**, 204701 (2006).
- <sup>2</sup>E. C. Le Ru, M. Meyer, and P. G. Etchegoin, *J. Phys. Chem. B* **110**, 1944 (2006).
- <sup>3</sup>P. J. G. Goulet and R. F. Aroca, *Anal. Chem.* **79**, 2728 (2007).
- <sup>4</sup>J. A. Dieringer, R. B. Lettan II, K. A. Scheidt, and R. P. Van Duyne, *J. Chem. Soc. A* **129**, 16249 (2007).
- <sup>5</sup>E. C. Le Ru, E. Blackie, M. Meyer, and P. G. Etchegoin, *J. Phys. Chem. C* **111**, 13794 (2007).
- <sup>6</sup>P. G. Etchegoin and E. C. Le Ru, *Phys. Chem. Chem. Phys.* **10**, 6079 (2008).
- <sup>7</sup>E. C. Le Ru and P. G. Etchegoin, *Principles of Surface-Enhanced Raman Scattering and Related Plasmonic Effects* (Elsevier, Amsterdam, 2009).
- <sup>8</sup>P. G. Etchegoin, M. Meyer, E. Blackie, and E. C. Le Ru, *Anal. Chem.* **79**, 8411 (2007).
- <sup>9</sup>Y. Fang, N.-H. Seong, and D. D. Dlott, *Science* **321**, 388 (2008).
- <sup>10</sup>J. Steidtner and B. Pettinger, *Phys. Rev. Lett.* **100**, 236101 (2008).
- <sup>11</sup>M. Meyer, E. C. Le Ru, and P. G. Etchegoin, *J. Phys. Chem. B* **110**, 6040 (2006).
- <sup>12</sup>S. Nie and S. R. Emory, *Science* **275**, 1102 (1997).
- <sup>13</sup>P. C. Lee and D. Meisel, *J. Phys. Chem.* **86**, 3391 (1982).
- <sup>14</sup>J. M. Gérardy and M. Ausloos, *Phys. Rev. B* **25**, 4204 (1982).
- <sup>15</sup>H. Xu, J. Aizpurua, M. Käll, and P. Apell, *Phys. Rev. E* **62**, 4318 (2000).
- <sup>16</sup>E. C. Le Ru and P. G. Etchegoin, *Chem. Phys. Lett.* **423**, 63 (2006).
- <sup>17</sup>E. C. Le Ru, J. Grand, N. Felidj, J. Aubard, G. Levi, A. Hohenau, J. R. Krenn, E. Blackie, and P. G. Etchegoin, *J. Phys. Chem. C* **112**, 8117 (2008).
- <sup>18</sup>E. C. Le Ru, M. Meyer, E. Blackie, and P. G. Etchegoin, *J. Raman Spectrosc.* **39**, 1127 (2008).